OPEN

Correspondence and requests for materials should be addressed to F.Y. (fanyang@stanford.edu)

Stem cells catalyze cartilage formation by neonatal articular chondrocytes in 3D biomimetic hydrogels

Janice H. Lai[1], Glen Kajiyama[2], Robert Lane Smith[2], William Maloney[2] & Fan Yang[2,3]

[1]Department of Mechanical Engineering, Stanford University, Stanford, CA 94305, USA, [2]Department of Orthopaedic Surgery, Stanford University, Stanford, CA, 94305, USA, [3]Department of Bioengineering, Stanford University, Stanford, CA, 94305, USA.

Cartilage loss is a leading cause of disability among adults and effective therapy remains elusive. Neonatal chondrocytes (NChons) are an attractive allogeneic cell source for cartilage repair, but their clinical translation has been hindered by scarce donor availability. Here we examine the potential for catalyzing cartilage tissue formation using a minimal number of NChons by co-culturing them with adipose-derived stem cells (ADSCs) in 3D hydrogels. Using three different co-culture models, we demonstrated that the effects of co-culture on cartilage tissue formation are dependent on the intercellular distance and cell distribution in 3D. Unexpectedly, increasing ADSC ratio in mixed co-culture led to increased synergy between NChons and ADSCs, and resulted in the formation of large neocartilage nodules. This work raises the potential of utilizing stem cells to catalyze tissue formation by neonatal chondrocytes via paracrine signaling, and highlights the importance of controlling cell distribution in 3D matrices to achieve optimal synergy.

Cartilage loss is a leading cause of disability among adults and represents a huge socio-economical burden. Articular cartilage has limited self-repair potential and damage is often irreversible[1]. Conventional cell-based therapy utilizes autologous chondrocytes for cartilage repair, which is associated with several shortcomings including donor site morbidity and the need for *in vitro* expansion and multiple surgeries[2]. Furthermore, the ability of autologous chondrocytes to regenerate cartilage tissue declines rapidly with patient age and *in vitro* expansion[3,4], making them a suboptimal cell source for cartilage repair. Unlike autologous adult chondrocytes, allogeneic neonatal chondrocytes (NChons) are highly proliferative, immune-privileged, and can readily produce abundant cartilage matrix[3,5,6]. However, donor availability for NChons is scarce, which greatly hinders their broad application.

In addition to chondrocytes, adult mesenchymal stem cells (MSCs) are an alternative cell source for cartilage repair[7]. Adipose-derived stem cells (ADSCs), in particular, are an attractive candidate due to their ease of isolation, relative abundance, and chondrogenic potential[8,9]. While stem cells are widely known for their potential to promote tissue regeneration through lineage-specific differentiation, emerging evidence suggests that paracrine signals secreted by stem cells may also contribute to tissue repair[10,11]. Several studies have examined the interactions between articular chondrocytes and MSCs; however, the reported results have been contradictory. While some studies indicated that MSCs inhibit cartilage production by chondrocytes[12,13], others showed that MSCs stimulate chondrocyte proliferation and cartilage matrix production[14–18]. The discrepant findings may be due to the differences in various parameters in these studies such as co-culture models, medium composition (i.e. serum or other growth factor supplementation), and donor age or disease phenotype of the chondrocytes. Furthermore, few studies have examined the interactions between ADSCs and NChons, and how their interactions affect cartilage formation remains largely unknown.

To study cell-cell interactions, several *in vitro* models have been developed including transwell co-culture, mixed cells plated in 2D or in a dense cell pellet. These models generally do not facilitate control over cell distribution and density, which in turn offer little control over the extent of cell-cell interactions. Moreover, studies have shown that chondrocytes de-differentiate rapidly in 2D and become more fibroblastic[19,20]. Therefore, novel co-culture models that better mimic physiologically relevant conditions are highly desirable for studying cell-cell interactions that involves chondrocytes. Unlike conventional *in vitro* co-culture models, biomimetic hydrogels provide a 3D microenvironment which allows for the retention of chondrocyte phenotype. Moreover,

hydrogels facilitate better control over cell density and distribution, which directly modulate local concentration of paracrine factors.

Here we examined the potential for ADSCs to catalyze cartilage tissue formation by a minimal number of NChons in 3D biomimetic hydrogels. To study the effects of interactions between ADSCs and NChons, we designed three *in vitro* co-culture models with varying cell distribution and intercellular distances in 3D hydrogels consisting of chondroitin sulfate methacrylate (CS-MA) and poly(ethylene) glycol diacrylate (PEGDA). CS is a constituent of aggrecan, a major proteoglycan found in cartilage. Such hydrogel composition mimics the function of native cartilage extracellular matrix (ECM), which provides a potential reservoir for secreted paracrine factors[21] and enables enzymatic degradation and matrix turnover by cell-secreted chondroitinase[22]. Furthermore, CS hydrogels have been shown to promote MSC chondrogenesis and may serve as potential scaffolding platform for cell delivery[22]. ADSCs and NChons were co-cultured in 3D hydrogels with varying spatial distribution under standard chondrogenic medium for three weeks. Outcomes were analyzed using quantitative gene expression, biochemical assays, and mechanical testing. The fate of each cell type and their respective contribution to the overall cartilage formation were identified using fluorescence-labeled cell tracking and immunofluorescence staining.

Results

Controlling cell distribution and intercellular distance in 3D biomimetic hydrogels. Using a 3D biomimetic hydrogel mimicking cartilage ECM, we encapsulated ADSCs and/or NChons using three *in vitro* co-culture models designed as following: 1) cells cultured with supplementation of conditioned medium (CM-) from the other cell type (Fig. 1A), 2) bi-layered (Bi-) co-culture confining each cell type to its own layer, with an acellular hydrogel interface (~250 μm thick) separating the two cell-containing layers (Fig. 1B), and 3) mixed co-culture of two cell types at different ratios (Fig. 1C). Cell viability was assessed 24 hours post-encapsulation, showing high cell viability (>90%) in all groups (Supplementary Fig. S1). Our co-culture models allow for control over cell distribution and intercellular distance in 3D, which is an important determinant in paracrine signaling as the concentration of paracrine factors decreases rapidly with increasing intercellular distance[23] (Fig. 1D). Previous study has suggested that 250 μm is the upper limit of intercellular distance for effective paracrine signal propagation[23]. To further examine the effects of intercellular distance on tissue formation, ADSC percentage was varied (25% to 90%) while the initial cell number was kept constant, which led to an increase in the number of ADSCs within the effective communication distance

of a NChon (Supplementary Fig. S2). The three co-culture models represented three scenarios with different cell distribution and extent of cell-cell interaction. In the conditioned medium model, cells interacted uni-directionally without dynamic exchange of paracrine signals. In bi-layered and mixed co-culture, the two cells types interacted bi-directionally with varying local paracrine signal concentration depending on the distribution of cells within the hydrogel matrix.

Mixed co-culture, but not conditioned medium or bi-layered co-culture, resulted in markedly enhanced ADSC chondrogenesis. To evaluate the effects of co-culture on cartilage-specific gene expression of ADSCs and NChons, species-specific primers were used to quantify the gene expression of aggrecan (Agg), type II collagen (COL2), and type I collagen (COL1). TGF-β3 induction led to marked increase in chondrogenic gene expression in ADSCs, confirming the chondrogenic potential of ADSCs (Supplementary Fig. S3, A and B). For the co-culture groups, ADSCs receiving conditioned medium (CM-ADSC) or maintained in bi-layered co-culture (bi-ADSC) showed only mild changes in chondrogenic marker expression together with a slight decrease in the fibroblastic marker COL1 (Fig. 2, A–C). In contrast, ADSCs cultured in all mixed co-culture groups showed markedly enhanced COL2 and Agg expression and the highest reduction in COL1 expression. Compared to ADSC control, Agg and COL2 expression in the mixed co-culture with varying ratios (25–90%) of ADSCs were 5.5–6 and 15.9–19 times (Fig. 2, A and B) higher respectively, while COL1 expression was decreased by 80% (Fig. 2C). Varying cell ratios in the mixed co-culture did not lead to significant changes in chondrogenic gene expression by ADSCs. Meanwhile, NChons in all three co-culture models largely maintained Agg and COL2 expression, with the exception of CM-treated NChons which had ~50% lower Agg expression compared to NChon control (Fig. 2, D and E; Supplementary Fig. S3, D and E). NChons in all the mixed co-culture groups except 10C:90A resulted in a 50% decrease in COL1 expression (Fig. 2F).

Mixed co-culture led to markedly increased cell proliferation, matrix production, and mechanical function of the newly formed cartilage. Could the three co-culture models also differentially impact cell proliferation and cartilage tissue formation? Next, we quantified DNA, cartilage-specific matrix content, and mechanical property of the resulting tissues at day 21. Gross appearance of the freeze-dried samples showed substantially increased tissue size in all the mixed co-culture groups and the NChon group after 21 days of culture, while tissue size decreased slightly in the ADSC control group (Supplementary Fig. S4). When cultured alone, the DNA content of ADSC control at day 21 decreased by 70% while NChon
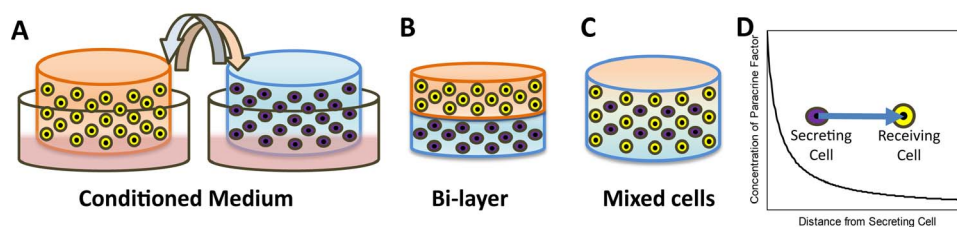

Figure 1 | Schematic representation of the experimental design. To examine the effects of intercellular distance and cell distribution on the interactions between adipose-derived stem cells (ADSCs) and neonatal articular chondrocytes (NChons), three different *in vitro* co-culture models were used: (A) In the condition medium (CM-) model, each cell type was cultured alone with supplementation of conditioned medium (CM) from the other cell type. (B) In the bi-layered (bi-) co-culture, ADSCs and NChons were confined in separate hydrogel layers with no direct cell-cell contact, and soluble paracrine signals were allowed to diffuse into the adjacent layer. (C) In the mixed cell co-culture model, ADSCs and NChons were mixed together in 3D at 4 different cell ratios (NChon:ADSC: 75C:25A, 50C:50A, 25C:75A, and 10C:90A). The initial cell density was maintained constant at 15 million/ml in all co-culture models. (D) The concentration of paracrine factors decays rapidly with distance from the secreting cell. In all the co-culture models, human adult ADSCs and bovine NChons were encapsulated in 3D biomimetic hydrogels and cultured *in vitro* for 21 days in chondrogenic medium supplemented with TGF-β3 (10 ng/ml).
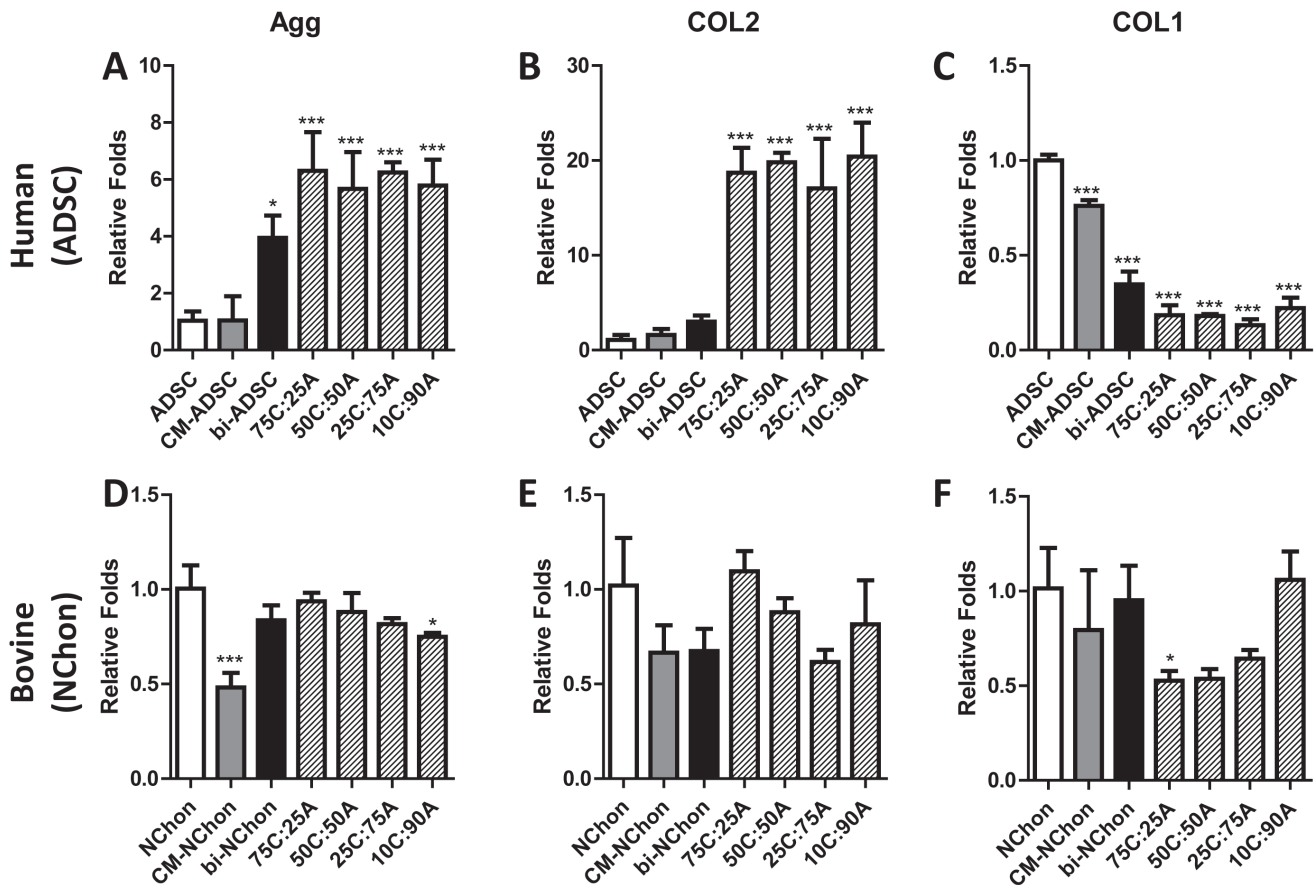
Figure 2 | Quantitative gene expression showed markedly enhanced ADSC chondrogenesis in mixed co-culture with all ratios, but not in conditioned medium or bi-layered co-culture. To distinguish the fate of each cell type, species-specific primers were used to identify the gene expression of human ADSCs and bovine NChons in the xenogenic co-culture. Human-specific (A–C) and bovine-specific (D–F) gene expression of (A, D) aggrecan (Agg), (B, E) type II collagen (COL II), and (C, F) type I collagen (COL I) after 21 days of *in vitro* co-culture in chondrogenic medium supplemented with TGF-β3. Fold changes relative to (A–C) ADSC and (D–F) NChon control at day 21. Data presented as mean +/− SD (n = 3 samples/group). Asterisks (*) indicate statistical significance between control (ADSC or NChon) and co-culture groups, with *P < 0.05, **P < 0.01, ***P < 0.001.

control showed 3-fold increase in DNA content compared to day 1. While conditioned medium and bi-layered co-culture led to a modest increase in ADSC proliferation, mixed co-culture led to the greatest increase (3–4 fold) in cell proliferation (Fig. 3A, Table S1). Sulfated glycosaminoglycan (sGAG) and total collagen content at day 21 showed similar trend as DNA content (Fig. 3, B and C). Mixed co-culture groups resulted in comparable sGAG (except for 10C:90A group) and higher collagen content compared to the NChon control. These values were significantly higher than those in the ADSC control. Only a mild increase in matrix production was observed in conditioned medium and bi-layered co-culture, with the bi-layered co-culture leading to more apparent increase than the conditioned medium group. Of all the cell ratios examined, the 50C:50A group had the greatest amount of collagen by day 21, which surpassed the positive control, NChon, by 30%. Mixed co-culture with as low as 25% NChons (25C:75A) also resulted in comparable sGAG content as the NChon control. When the percentage of NChons in mixed co-culture was further reduced (10C:90A), sGAG and collagen content dropped to ~60–70% of the NChon control (Fig. 3, B and C). In addition to biochemical content, the functional property of neo-cartilage was quantified using unconfined compression test at the end of 21-day culture. Compressive moduli in NChon control and all the mixed cell groups increased up to 2.65 folds over 21 days (Fig. 3D, Table S2) whereas no significant changes were observed in ADSC control. Compressive modulus was the highest in the NChon control and decreased progressively with an increase in ADSC ratio in the mixed cell population.

The extent of enhanced cartilage tissue production is dependent on cell ratio in mixed co-culture. To further elucidate the effects of varying cell ratio on cell interactions, we calculated the interaction index of DNA, sGAG, and collagen content using a method previously reported by Acharya et al.[14]. The interaction index is defined as the measured value of DNA, sGAG, or collagen content in the mixed co-culture normalized by the expected value based on the ratio and the measured value when each cell type is cultured alone. The interaction index for DNA, sGAG, and collagen per wet weight in all the mixed co-culture groups were higher than 1 (Fig 3, E–G). In addition, the interaction index increased as the ratio of ADSCs increased. At 90% ADSC (10C:90A), DNA, sGAG, and collagen content were approximately 5–6 fold higher than expected. When normalized by DNA, the interaction index for sGAG and collagen was close to 1 (Table S3).

The nodule size of newly formed cartilage increased with an increase in the ratio of stem cells in the mixed co-culture. To gain insight into the effect of co-culture models on spatial organization of neo-cartilage formation over time, we performed immunostaining of type I, II, and X collagen on tissue sections harvested at day 7, 14 and 21. While no apparent changes were induced by conditioned medium or bi-layered co-culture, formation of large cartilage nodules was observed in mixed co-culture, with marked difference in neo-cartilage organization as a result of varying cell ratio. While cells remained mostly as single cells in hydrogels at day 7, cell aggregates and neo-cartilage nodules started to emerge by day 14
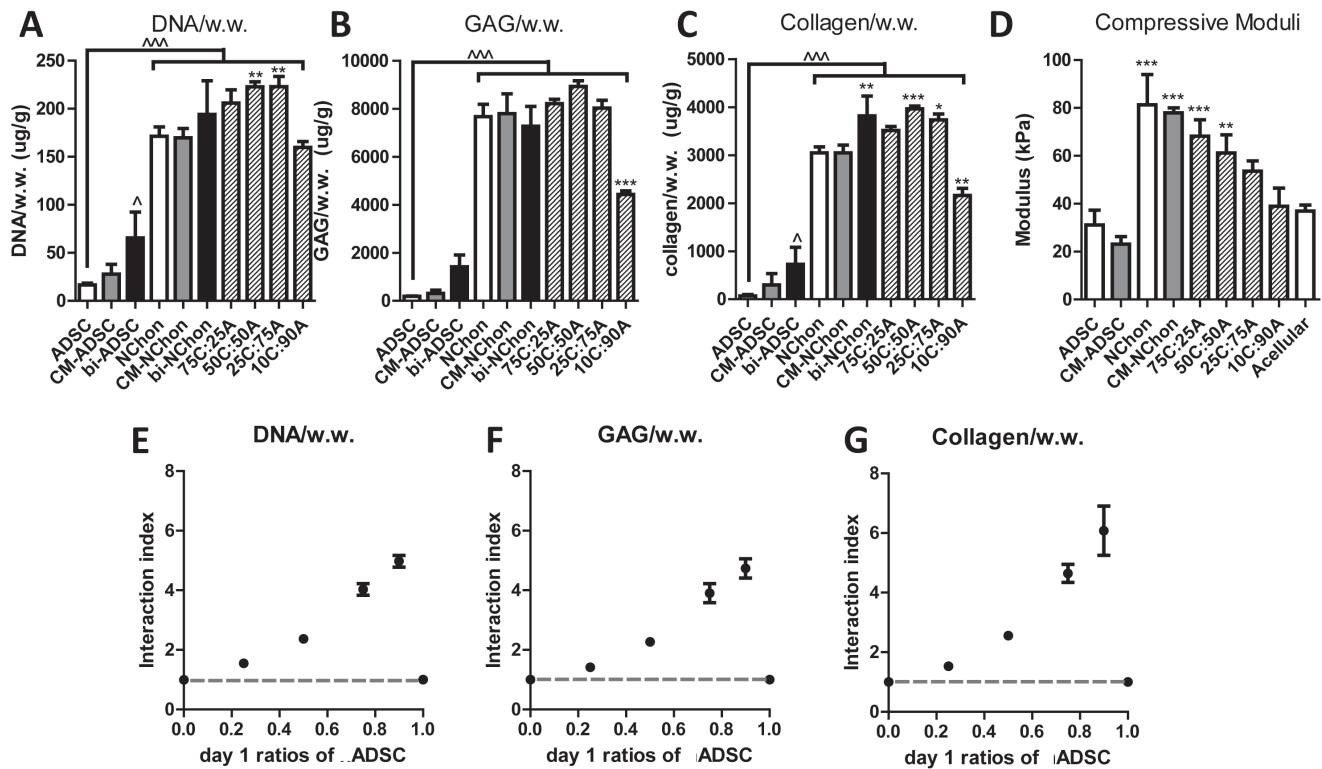
Figure 3 | Biochemical assays and mechanical testing showed that enhanced cell proliferation, cartilage matrix production, and mechanical property in the mixed co-culture, but not in conditioned medium or bi-layered co-culture. Such synergy increased as ratio of ADSC increased in the mixed co-culture. (A) DNA, (B) glycosaminoglycan (GAG), and (C) collagen per wet weight (w.w.) after 21 days of culture. (D) Compressive tangent moduli of tissue-engineered constructs at day 21. Data was presented as mean $+/-$ SD (n = 4 samples/group). To quantify the synergy between ADSCs and NChons during mixed co-culture, interaction index was calculated as the measured matrix content at various cell ratios normalized by the expected matrix content given no interaction between the two cell types. Interaction index for (E) DNA/w.w., (F) GAG/w.w., and (G) collagen/w.w. increased with an increase in ADSC ratio in the mixed cell co-culture. (*) indicates statistical significance against NChon control and (^) indicates statistical significance against ADSC control, with *P < 0.05, **P < 0.01, ***P < 0.001.

(Supplementary Fig. S5) and continued to increase in size up to day 21 (Fig. 4A, Supplementary Fig. S6). Increasing ADSC ratio led to an increase in the individual nodule size as well as the total area occupied by the nodules (Fig. 4, C–E). By day 21, the average nodule size in the group with 90% ADSCs (10C:90A) was 6 times larger than that in NChon control with extensive matrix remodeling. Meanwhile, minimal amount of type I and type X collagen was detected in all groups at day 21 as shown by immunofluorescence staining (Supplementary Fig. S7).

ADSCs catalyzed neocartilage formation by NChons via paracrine signaling. To identify the relative contribution of each cell type to neocartilage nodule formation in mixed co–culture, ADSCs were fluorescently labeled prior to encapsulation in the mixed co-culture with un-labeled NChons. Cell tracking along with co-localization of collagen II immunostaining demonstrated that fluorescently labeled ADSCs always resided outside the cell aggregates and newly formed cartilage nodules (Fig. 4B), indicating that the newly formed cartilage nodules were produced entirely by NChons. No direct cell-cell contact between the two cell types was observed.

Close proximity between NChons and ADSCs was crucial for synergistic interactions. To further examine the role of proximity between the two cell types on cartilage matrix production, we examined cartilage formation at the interface of bi-layered co-culture, with or without an acellular hydrogel layer ($\sim$250 μm) using collagen type II immunostaining. As shown in Fig. 5A, large cartilage nodules were localized at the interface of the NChons and ADSCs in the absence of an intermediate acellular hydrogel layer

with a thickness of $\sim$250 μm. In contrast, when the two cellular layers were separated by an acellular hydrogel layer, no large cartilage nodule was observed at the interface (Fig. 5B).

Discussion

In this study, we demonstrated the feasibility of minimizing the number of NChons needed for cartilage regeneration by exploiting cell-cell interactions between ADSCs and NChons using 3D biomimetic hydrogels. Our findings suggested the possibility of overcoming one major bottleneck that hinders the broad clinical application of NChons, namely, donor scarcity despite their high proliferative and cartilage regenerative potential. By exploiting the paracrine signals from stem cells and controlling cell distribution in 3D co-culture, we demonstrated that robust cartilage tissue formation can be achieved using as low as 10% of NChons in mixed co-culture with ADSCs. While a few recent studies have shown that co-culture of stem cells and chondrocytes in 3D resulted in enhanced cartilage formation[16,24], our study is the first report that such synergistic interaction is highly dependent on the spatial distribution and distance between the two cell types. Only mixed co-culture, but not bi-layered or conditioned medium, resulted in robust synergistic interaction between ADSCs and NChons. This trend was consistent in all assays performed including upregulated chondrogenic gene expression, increased cell proliferation and cartilage matrix deposition, and enhanced compressive moduli of the tissue-engineered constructs at day 21. In contrast, conditioned medium and bi-layered co-culture only had mild effects on cell fate and cartilage tissue formation. Together with the localized formation of cartilage nodules at the interface in bi-layered co-culture in the absence of an intermediate
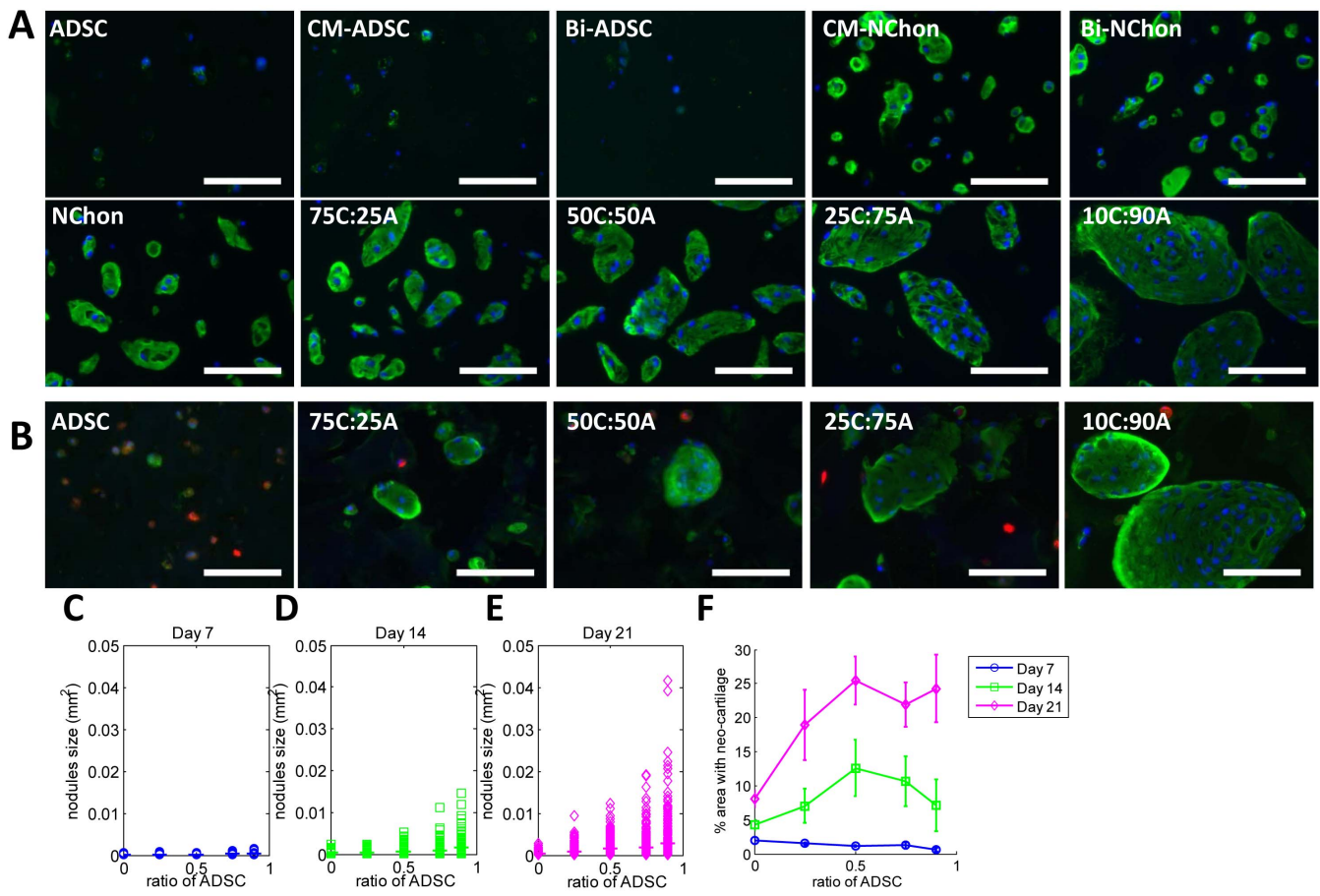
Figure 4 | The morphology of newly formed cartilage nodules and cell distribution over 21 days. (A) Newly formed cartilage nodules were visualized by immunostaining of type II collagen at day 21. Scale bars, 100 μm. (B) To determine the distribution of the two cell types in the mixed cell culture, ADSCs were membrane-labeled (red) prior to encapsulation in the hydrogels; co-staining with type II collagen (green) revealed that ADSCs always resided outside the neocartilage nodules. Scale bars, 100 μm. (C–F) Quantification of type II collagen immunostaining images, including cartilage nodule size at different ratios of ADSCs at (C) day 7, (D) day 14, and (E) day 21 (horizontal bars indicate average size), as well as the (F) total percentage of area occupied by cartilage nodules at different cell ratios at day 7, 14, and 21. Both the cartilage nodule size as well as the total area of hydrogel being replaced by cartilage nodules increased with an increase in ADSC ratio in the mixed co-culture.

acellular layer, these findings strongly suggested that close proximity between the two cell types was crucial for such synergistic interaction. Unexpectedly, the degree of synergistic interaction, as indicated by interaction index, increased with an increase in ADSC ratio in mixed co-culture. This finding may have significant impact on accelerating the use of allogeneic neonatal chondrocytes for cartilage repair, as the majority of NChons may be substituted with ADSCs, an easily accessible and abundantly available autologous cell source. By harnessing their synergistic interactions with ADSCs, the same number of available NChons may be used to treat more patients.

While previous studies have focused on examining interactions between MSCs and adult chondrocytes, little is known about how ADSCs and NChons interact during cartilage formation[14–16,18,24–29]. Our study filled this critical void of knowledge by providing comprehensive analyses of ADSC-NChon interactions using biomimetic hydrogels with control over cell distribution in 3D. Furthermore, previous studies have concluded different mechanisms and the fate of each cell type during co-culture. While some studies suggested that MSCs stimulated chondrocytes to proliferate and form cartilage tissues via trophic factors[14,15] such as fibroblast growth factor-1 (FGF-1)[30], other studies concluded that such enhanced cartilage formation was mainly contributed by MSC chondrogenesis, which was stimulated by chondrocytes via paracrine signaling[25,26]. Similarly, mixed results have been reported for ADSC-chondrocyte interactions.

Some showed that ADSCs positively enhance chondrocyte proliferation and cartilage matrix synthesis[14,27,31], while others showed that ADSCs inhibited chondrocyte proliferation and led to the formation of fibrocartilage tissue[32,12]. Such inconsistency in previous findings was likely due to the lack of control over cell distribution and the extent of cell-cell interaction in co-culture models such as pellet or trans-well co-culture. In pellet co-culture, cells were packed densely with direct cell-cell contact, making it difficult to control intercellular distance. In pre-fabricated scaffolds such as PCL scaffold, cells were seeded on top of the scaffold post-fabrication and cells may aggregate and distribute unevenly within the scaffold during the seeding process. In contrast, our 3D biomimetic hydrogels allowed cells to be evenly distributed throughout the matrix with control over cell density and distribution. Furthermore, this is the first study to systematically compare various co-culture models using 3D biomimetic hydrogels (conditioned medium, bi-layered, and mixed co-cultures at different cell ratios). We also examined in depth the effects of changing cell ratio across a broad range in mixed co-culture on the extent of cartilage formation. A recent study by Bian et al.[24] examined the effects of varying cell ratios of osteoarthritic chondrocytes and BMSCs using hyaluronic acid hydrogels, and showed enhanced cartilage formation can be achieved using as few as 20% OA chondrocytes in the mixed co-culture. The authors concluded that such cartilage formation was contributed mostly by MSC chondrogenesis stimulated by chondrocytes. In contrast, our cell
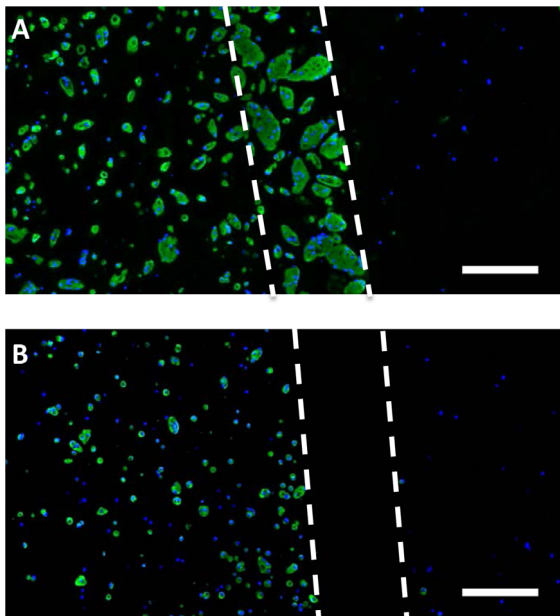
Figure 5 | Large cartilage nodule formation was localized at the interface of the two cells and only occurred in the absence an acellular intermediate hydrogel layer. Newly formed cartilage nodules were visualized by immunostaining of type II collagen at day 21 in bi-layered co-culture (A) in the absence of an intermediate acellular hydrogel layer and (B) with a 250 μm acellular layer. Scale bars, 200 μm. Dotted lines in (A) indicate the localization of large cartilage nodules at the bi-layer interface, and in (B), the acellular intermediate layer.

tracking results and interaction index analyses suggested a different mechanism for such enhanced cartilage formation during co-culture, namely, ADSCs catalyzed NChons to proliferate and deposit articular cartilage matrix via paracrine signaling, and such synergy increased in a dose-dependent manner even using as few as 10% NChons.

Different from the previous reports, we co-cultured ADSCs and NChons in three *in vitro* co-culture models using 3D biomimetic hydrogels in order to systematically examine the role of cell distribution and intercellular distance on cell-cell interactions. Such hydrogels were photo-crosslinked and allowed for better control over cell density and distribution in 3D compared to cell pellets and porous scaffolds. Furthermore, the hydrogel contained chondroitin sulfate and has been shown to enhance chondrocyte phenotype as well as MSC chondrogenesis *in vitro*[22,33]. Three co-culture models were used. Conditioned medium represented paracrine signaling without dynamic crosstalk between the two cell types. The bi-layered co-culture model represented a gradient of paracrine signal concentration, as the two cell types were confined to separate hydrogel layers which were either placed adjacent to each other or physically separated by an acellular hydrogel interface of 250 μm thickness, which is comparable to the previously reported paracrine signal propagation limit. The mixed co-culture model allowed for the two cell types to interact at close proximity, and represented an environment with the highest available local paracrine signaling. By varying the cell ratio in mixed co-culture and performing detailed analyses including interaction index as well as quantitative characterization of cartilage nodule formation over time, our study highlighted the importance of cell-cell proximity on interaction synergy.

To elucidate the respective contribution of each cell type, we employed a xenogenic co-culture using human ADSCs and bovine NChons together with species-specific primers to identify gene expression of each cell type in co-culture. Bovine chondrocytes have been widely used for such studies given the abundance of bovine

cartilage tissue from different ages (especially juvenile)[34–36]. Several co-culture studies have utilized human BMSCs and bovine chondrocytes and confirmed primer specificity for such xenogenic co-culture to track species-specific cell fate[14,15,28]. In addition, previous studies have also shown that trends observed in human-human and human-bovine co-culture studies were consistent, both exhibiting synergistic interactions with enhanced chondrocyte proliferation and cartilage matrix production. We further utilized fluorescence-labeled cell tracking to locate the distribution of ADSCs and NChons within the hydrogel matrix and identify their relative contribution to cartilage matrix formation over time. Such membrane labeling dye has been previously used for long-term cell tracking both *in vitro* and *in vivo*[37,38], and divides between cells during cell division[39].

The fact that enhanced cartilage tissue formation was observed only in mixed co-culture suggested that spatial distribution of the two cell types in 3D was critical for such catalyzed tissue formation. Meanwhile, despite the markedly enhanced cell proliferation, NChons maintained their chondrocyte phenotype as shown by cartilage-specific gene expression and immunofluorescence staining. One remarkable finding of our study was that mixed co-culture with as low as 25% NChons resulted in an overall increase in sGAG content to a level that was comparable and DNA and collagen content that even surpassed the positive control group comprised of 100% NChons, which are known for their capacity of active proliferation and cartilage matrix production[4]. Type I and X collagen staining was minimal (Supplementary Fig. S7), indicating that the newly formed cartilage tissues did not contain fibroblastic or hypertrophic phenotype, and is suitable for articular cartilage repair. In contrast, only mild changes were observed in the bi-layered and conditioned medium co-culture. Furthermore, when the ADSCs and NChons layers were directly next to each other, cartilage nodule formation was observed at the interface of the bi-layered co-culture, which spanned approximately 250 μm in distance. Interestingly, when the two cell-containing layers were physically separated by a thin layer of acelluar gel with a thickness of around 250 μm, no large cartilage nodule was observed. Together, these results strongly suggested that the two cell types must reside within certain distance to each other to achieve a threshold of paracrine signaling for such synergy to occur. Through examining the spatial organization of cartilage nodules in various co-culture models in 3D biomimetic hydrogels, we have demonstrated the importance of intercellular distance on interaction synergy and the resulting neocartilage formation. To further examine the effects of intercellular distance and spatial distribution on cell-cell interactions, other micropatterning techniques such as soft lithography, stereolithography, and microfluidics may be employed to achieve more refined control over cell distribution in 3D[40,41].

Our results also showed that the degree of synergy was highly dependent on the cell ratio in mixed co-culture. The interaction index, which is a quantification of synergy, increased with an increase in ADSC ratio for DNA, sGAG, as well as collagen content, and reached up to 5–6 at 90% ADSCs (Fig. 3E–G). The interaction index for sGAG and collagen, when normalized by DNA, was close to 1 at all cell ratios. This indicated that enhanced total cartilage matrix production was contributed by enhanced cell proliferation, but not matrix production per cell. Similar to the increase in interaction index, the size of the cartilage nodules also increased with an increase in ADSC ratio, which was likely a result of increased concentration of paracrine factors secreted by ADSCs.

Previous studies have shown that increase in cell proliferation is generally accompanied by decrease in the matrix production per cell[42]. Remarkably, our results showed that NChons were able to maintain their capacity of producing cartilage matrix actively while increasing cell proliferation as a result of mixed cell co-culture. Although the total sGAG and collagen content in 10C:90A was not the highest at day 21, the increased synergy with an increase in ADSC

ratio suggested that 10C:90A group may surpass that of NChon given longer culture period, and that the minimal number of NChons needed in the mixed co-culture may be further reduced for robust cartilage formation.

While both interaction index and cartilage nodule size were the highest in 10C:90A group, total collagen content in 10C:90A was significantly lower than NChon control. Total collagen content was quantified with hydroxyproline assay, which measured all collagen types (including type I and X). Immunostaining results showed intense staining for collagen type II and minimal staining for collagen type I and X in all samples. It was likely that although nodule size and total area of nodule formation was high in 10C:90A group, the density of cartilage matrix in the nodules was lower in this group. Lower compressive moduli were observed in mixed co-culture groups with higher ADSC ratios in spite of the formation of large cartilage nodules and comparable sGAG and collagen content. This also suggested that the cartilage matrix density of the newly formed cartilage nodules might be lower in mixed co-culture groups. In addition, the differences in cartilage nodule size and distribution as well as remodeling of the hydrogel scaffolds may also contribute to the differences in compressive moduli in the mixed co-culture groups compared to the NChon control.

What was the relative contribution of each cell type to cartilage nodule formation in mixed co–culture? Cell tracking along with co-localization of collagen II immunostaining demonstrated that fluorescently labeled ADSCs always resided outside the cell aggregates and newly formed cartilage, suggesting that NChons were responsible for the newly formed cartilage nodules. The sparsity of the fluorescently labeled ADSCs suggested that they died off over time in mixed co-culture. This is consistent with the ADSC control which showed ~70% decrease in DNA content after 21 days of *in vitro* culture. Similarly, previous studies on chondrogenesis of MSCs have shown increased cell apoptosis over time both when cultured alone[43,44] or during mixed co-culture with chondrocytes[15,16]. Furthermore, although ADSC chondrogenesis was enhanced at the gene expression level, immunostaining results indicated that the fluorescently labeled ADSCs produced little collagen type II. This suggested that while ADSCs underwent chondrogenesis during the co-culture, it was not sufficient for extensive cartilage matrix deposition. In addition, cell labeling showed that the newly formed cartilage nodules were composed of NChons alone, and that ADSCs mainly contributed to the enhanced matrix production through their paracrine effects on NChons.

Different from the trend observed in the mixed co-culture groups, conditioned medium resulted in minimal synergistic or even negative interaction (CM-NChon showed 50% lower Agg expression). Given that the two cell types never interacted bi-directionally in the conditioned medium group, these results suggested that dynamic interaction with the presence of both cell types may be essential for synergistic interaction to occur. Similar to our findings, Aung et al. showed that conditioned medium from chondrocytes inhibited chondrogenesis of bone marrow-derived MSCs, whereas transwell co-culture resulted in enhanced chondrogenesis[18].

While many cell-based therapies harness the ability of stem cells to differentiate and produce specific tissue types to achieve tissue regeneration, mounting evidence suggests that stem cells may also contribute to tissue regeneration through paracrine effects. In wound healing, it has been shown that BMSCs may contribute through releasing paracrine signals to recruit endogenous macrophages and endothelial progenitor cells[45]; in myocardial infarction, it has been shown that transplanted BMSCs enhance vascular regeneration through the secretion of angiogenic factors[46]. ADSCs secrete a broad spectrum of paracrine signals that are known to stimulate cell proliferation including fibroblast growth factor-2 (FGF-2), vascular endothelial growth factor (VEGF), and insulin-like growth factor 1(IGF-1)[47,48]. Of these factors, FGF-2 and IGF-1 have also been shown to induce GAG and type II collagen synthesis in chondrocytes[49], while FGF-2 may reduce fibroblastic and hypertrophic phenotype in chondrocytes[50,51]. The paracrine signals released by the stem cells may also change as they differentiate[52]. Pre-differentiation of BMSCs towards osteogenic lineage has been shown to enhance their capacity to stimulate cartilage tissue formation by chondrocytes[53]. In our co-culture model, ADSCs underwent chondrogenesis under TGF-β3 induction. Type II collagen immunostaining indicated that cartilage nodules started to emerge after day 7. The delayed emergence of cartilage nodules suggested that ADSCs may need to partially differentiate towards chondrogenesis for robust synergy to occur, and that both ADSCs and NChons may dynamically change their paracrine factor profile over time.

In sum, here we demonstrated the efficacy of harnessing the paracrine effects of ADSCs to catalyze cartilage tissue formation by a small number of allogeneic neonatal chondrocytes (NChons) in biomimetic hydrogels. The differential effects of various co-culture models on cartilage tissue formation highlighted the importance of using 3D scaffolds to probe cell-cell interactions in a spatially controlled manner. These 3D co-culture models are not only a valuable tool for studying cell-cell interactions but may provide potential strategies to enhance cell-based therapy for tissue regeneration by harnessing the synergistic effects of cell-cell interaction. Our results showed that by modulating NChon-ADSC interactions in 3D, it is possible to significantly reduce the number of NChons needed for cartilage regeneration, which may accelerate the broad translation of NChons for cartilage repair by alleviating the donor scarcity limitation. Finally, the concept of harnessing the paracrine signaling between two or more cell types in 3D scaffolds to catalyze tissue formation may be broadly applicable to regenerating other tissue types as well.

Methods
All experimental protocols reported were approved by Stanford University.

Cell isolation and culture. *Chondrocytes.* Hyaline articular cartilage was dissected from the femoropatellar groove of two stifle joints from a three-day old calf (Research 87, Marlborough, MA). The cartilage was sliced into thin pieces and digested in 1 mg/mL collagenase type II and type IV (Worthington Biochemical, Lakewood, NJ) in high glucose DMEM (Gibco, Invitrogen, Carlsbad, CA) supplemented with 100 U/mL penicillin and 0.1 mg/mL streptomycin (Gibco, Invitrogen, Carlsbad, CA) for 24 hours at 37°C. The cell suspension was filtered through a 70 µm nylon mesh, centrifuged and washed in DPBS, and counted with a hemocytometer. The neonatal chondrocytes (NChons) were then suspended in freezing media (DMEM supplemented with 10% dimethyl sulfoxide (DMSO, Fisher Scientific, Pittsburgh, PA) and 50% fetal bovine serum (FBS, Gibco, Invitrogen, Carlsbad, CA), frozen at 1°C/min, and stored in liquid nitrogen.

Adipose-derived stem cells. Human adult adipose-derived stem cells (ADSCs) were isolated from excised human adipose tissue with informed consent as previously described[9]. ADSCs were expanded for 4 passages in high glucose DMEM supplemented with 5 ng/mL basic fibroblast growth factor (bFGF), 100 U/mL penicillin, and 0.1 mg/mL streptomycin.

3D hydrogel co-culture. On the day of cell encapsulation, NChons were thawed, recounted and used without further expansion. Cells were suspended at 15×10^6 cells/mL in a hydrogel solution consisted of 7% weight/volume (w/v) poly(ethylene glycol) diacrylate) (PEGDA, MW = 5000 g/mole), 3% w/v chondroitin sulfate-methacrylate (CS-MA), and 0.05% w/v photoinitiator (Irgacure D 2959, Ciba Specialty Chemicals, Tarrytown, NY) in DPBS. The cell-hydrogel suspension was pipetted into a custom-made cylindrical gel mold with 75 µl volume and exposed to UV light (365 nm wavelength) at 3 mW/m² for 5 minutes to induce gelation. To create bi-layered hydrogel, cell-hydrogel suspension (37.5 µl each) of one cell type was deposited into the cylindrical gel mold and photo-crosslinked before deposition of the next cell-hydrogel layer. To prevent direct cell-cell contact, the two cell-hydrogel layers were separated by an acellular hydrogel interface (10 µl). The duration of UV exposure for the three sequential layers was 3, 2, and 5 minutes.

Co-culture models. To examine the effects of different local paracrine signal concnetrations on cell fate, NChons and ADSCs were co-cultured in three different co-culture models: 1) cells cultured with supplementation of conditioned medium from the other cell type (Fig. 1A), 2) bi-layered co-culture confining each cell type to its own layer, with an acellular hydrogel interface (~250 µm thick) separating the two cell-containing layers (Fig. 1B), and 3) mixed co-culture of two cell types at different

ratios (75C:25A, 50C:50A, 25C:75A, 10C:90A) (Fig. 1C). Conditioned medium was collected every two days, filtered through a 0.2 μm mesh, and diluted with an equal volume of fresh chondrogenic medium. All samples were cultured in chondrogenic medium (high-glucose DMEM (Gibco, Invitrogen, Carlsbad, CA) containing 100 nM dexamethasone (Sigma-Aldrich, St. Louis, MO), 50 μg/ml ascorbate-2-phosphate (Sigma-Aldrich, St. Louis, MO), 40 μg/ml proline (Sigma-Aldrich, St. Louis, MO), 100 μg/ml sodium pyruvate (Gibco, Invitrogen, Carlsbad, CA), 100 U/mL penicillin, 0.1 mg/mL streptomycin, and ITS Premix (5 μg/ml insulin, 5 μg/ml transferrin, 5 ng/ml selenious acid, BD Biosciences, San Jose, CA) supplemented with 10 ng/ml TGF-β3 (PeproTech, Rocky Hill, NJ) for 3 weeks.

Gene expression analysis. Total RNA was extracted from cell-hydrogel constructs (n = 3) using TRIzol (Invitrogen, Carlsbad, CA) and the RNeasy mini kit (Qiagen, Valencia, CA). One mg of RNA from each sample was reversed transcribed into cDNA using the Superscript First-Strand Synthesis System (Invitrogen, Carlsbad, CA). Real-time polymerase chain reaction (PCR) was performed on an Applied Biosystems 7900 Real-Time PCR system using SYBR green master mix (Applied Biosystems, Carlsbad, CA) and primers listed in Table S4. Human- and bovine-specific primers were used to quantify gene expression of chondrogenic markers including Type II collagen (COL2) and aggrecan (Agg) as well as fibroblastic marker type I collagen (COL1) using $\delta\delta Ct$ method[54]. Gene expression levels were normalized internally to GAPDH. Relative fold changes represent changes in gene expression compared with NChon control group (for bovine-specific gene expression) and ADSCs control group (for human-specific gene expression) at day 21.

Biochemical analysis. Cell-hydrogel constructs (n = 4) were weighed wet, lyophilized, weighed dry, and digested in papainase solution (Worthington Biochemical, Lakewood, NJ) at 60°C for 16 hours. DNA content was measured using the PicoGreen assay (Molecular Probes, Eugene, OR) using Lambda phage DNA as standard. Sulfated glycosaminoglycan (sGAG) content was quantified using the 1,9-dimethylmethylene blue (DMMB) dye-binding assay with shark chondroitin sulfate (Sigma, St. Louis, MO) as standard[55]. Total collagen content was determined using acid hydrolysis followed by reaction with p-dimethylaminobenzaldehyde and chloramine T (Sigma, St. Louis, MO). Collagen content was estimated by assuming 1 : 7.46 hydroxyproline:collagen mass ratio[56,57]. The interaction index, which is the measured matrix content (DNA, sGAG, or collagen) in the mixed co-culture group normalized by the expected matrix content based on the measured matrix content per wet weight in the NChon and ADSC control groups, was calculated[14]. An interaction index of greater than 1 indicates that the resulting matrix content is higher than expected.

Histological analysis. Cell-hydrogel constructs (n = 2) were fixed in 4% paraformaldehyde (Sigma, St. Louis, MO) overnight and stored in 70% ethanol at 4°C until processed. Constructs were then embedded in paraffin and processed using standard histological procedures. For immunostaining, enzymatic antigen retrieval was performed by incubation in 0.1% trypsin (Gibco, Invitrogen, Carlsbad, CA) at 37°C for 15 minutes. Sections were then blocked with blocking buffer consisting of 2% goat serum (Gibco, Invitrogen, Carlsbad, CA), 3% BSA (Fisher Scientific, Pittsburgh, PA) and 0.1% Triton X-100 (Sigma, St. Louis, MO) in 1× PBS, followed by incubation in rabbit polyclonal antibody to collagen type I, II, or X (Abcam, Cambridge, MA) overnight at 4°C and secondary antibody (Alexa Fluor 488 goat anti-rabbit, Invitrogen, Carlsbad, CA) incubation for an hour at room temperature. Nuclei were counterstained with DAPI mounting medium (Vectashield, Vector Laboratories, Burlingame, CA) and images were taken with a Zeiss fluorescence microscope. Sections without primary antibody incubation serve as negative controls. A custom image processing program was written in MATLAB (The MathWorks, Natick, MA) to quantify the number and size of the cartilage nodules.

Cell tracking using membrane labeling. To track cell distribution within the hydrogel constructs over time, ADSCs were labeled with red fluorescent dye (PKH26, Sigma, St. Louis, MO) prior to encapsulation at a concentration of 4 μM for 4 minutes following manufacturer's protocol. Labeled ADSCs were encapsulated with NChons in the mixed co-culture hydrogel model at different cell ratios for 21 days (n = 3). Samples were fixed in 4% paraformaldehyde (Sigma, St. Louis, MO) overnight, submerged in 30% sucrose (Sigma, St. Louis, MO) solution for 24 hours, embedded in Tissue-Tek (Sakura Finetek, USA), and frozen in liquid nitrogen. Cryosections (12 μm-thick) were washed in DPBS and collagen II and cell nuclei were stained using the immunostaining procedures described above.

Mechanical testing. Unconfined compression tests were conducted using an Instron 5944 materials testing system (Instron Corporation, Norwood, MA) fitted with a 10 N load cell (Interface Inc., Scottsdale, AZ). Cell-hydrogel constructs were tested on day 1 and day 21 of culture (n = 4). During testing, cell-hydrogel constructs were submerged in a PBS bath at room temperature. Constructs was compressed at a rate of 1% strain/sec to a maximum strain of 15%. Stress vs. strain curves were created and curve fit using a third order polynomial equation. The compressive tangent modulus was determined from the curve fit equation at strain values of 15%.

Statistical analysis. GraphPad Prism (Graphpad Software, San Diego, CA) was used to perform statistical analysis. One- or two-way analysis of variance and pairwise comparisons with Tukey's post-hoc test were used to determined statistical significance ($p < 0.05$). Data was represented as mean ± standard deviation of at least three biological replicates.

1. Griffin, T. M. & Guilak, F. The role of mechanical loading in the onset and progression of osteoarthritis. *Exerc Sport Sci Rev* **33**, 195–200 (2005).
2. Brittberg, M. *et al.* Treatment of deep cartilage defects in the knee with autologous chondrocyte transplantation. *N Engl J Med* **331**, 889–95 (1994).
3. Adkisson, H. D. *et al.* The potential of human allogeneic juvenile chondrocytes for restoration of articular cartilage. *Am J Sports Med* **38**, 1324–33 (2010).
4. Saha, S., Kirkham, J., Wood, D., Curran, S. & Yang, X. Comparative study of the chondrogenic potential of human bone marrow stromal cells, neonatal chondrocytes and adult chondrocytes. *Biochem Biophys Res Commun* **401**, 333–8 (2010).
5. Adkisson, H. D., Gillis, M. P., Davis, E. C., Maloney, W. & Hruska, K. A. In vitro generation of scaffold independent neocartilage. *Clin Orthop Relat Res*, S280–94 (2001).
6. Adkisson, H. D. *et al.* Immune evasion by neocartilage-derived chondrocytes: Implications for biologic repair of joint articular cartilage. *Stem Cell Res* **4**, 57–68 (2010).
7. Pittenger, M. F. *et al.* Multilineage potential of adult human mesenchymal stem cells. *Science* **284**, 143–7 (1999).
8. Guilak, F., Awad, H. A., Fermor, B., Leddy, H. A. & Gimble, J. M. Adipose-derived adult stem cells for cartilage tissue engineering. *Biorheology* **41**, 389–99 (2004).
9. Zuk, P. A. *et al.* Multilineage cells from human adipose tissue: implications for cell-based therapies. *Tissue Eng* **7**, 211–28 (2001).
10. Caplan, A. I. & Dennis, J. E. Mesenchymal stem cells as trophic mediators. *J Cell Biochem* **98**, 1076–84 (2006).
11. Gnecchi, M., Zhang, Z., Ni, A. & Dzau, V. J. Paracrine mechanisms in adult stem cell signaling and therapy. *Circ Res* **103**, 1204–19 (2008).
12. Lee, C. S. *et al.* Adipose stem cells can secrete angiogenic factors that inhibit hyaline cartilage regeneration. *Stem Cell Res Ther* **3**, 35 (2012).
13. Xu, L. *et al.* Mesenchymal Stem Cells Downregulate Articular Chondrocyte Differentiation in Noncontact Coculture Systems: Implications in Cartilage Tissue Regeneration. *Stem Cells Dev* **22**, 1657–69 (2013).
14. Acharya, C. *et al.* Enhanced chondrocyte proliferation and mesenchymal stromal cells chondrogenesis in coculture pellets mediate improved cartilage formation. *J Cell Physiol* **227**, 88–97 (2012).
15. Wu, L. *et al.* Trophic effects of mesenchymal stem cells increase chondrocyte proliferation and matrix formation. *Tissue Eng Part A* **17**, 1425–36 (2011).
16. Meretoja, V. V., Dahlin, R. L., Kasper, F. K. & Mikos, A. G. Enhanced chondrogenesis in co-cultures with articular chondrocytes and mesenchymal stem cells. *Biomaterials* **33**, 6362–9 (2012).
17. Hwang, N. S. *et al.* Chondrogenic priming adipose-mesenchymal stem cells for cartilage tissue regeneration. *Pharm Res* **28**, 1395–405 (2011).
18. Aung, A., Gupta, G., Majid, G. & Varghese, S. Osteoarthritic chondrocyte-secreted morphogens induce chondrogenic differentiation of human mesenchymal stem cells. *Arthritis Rheum* **63**, 148–58 (2011).
19. Holtzer, H., Abbott, J., Lash, J. & Holtzer, S. THE LOSS OF PHENOTYPIC TRAITS BY DIFFERENTIATED CELLS IN VITRO, I. DEDIFFERENTIATION OF CARTILAGE CELLS. *Proc Natl Acad Sci U S A* **46**, 1533–42 (1960).
20. Darling, E. M. & Athanasiou, K. A. Rapid phenotypic changes in passaged articular chondrocyte subpopulations. *J Orthop Res* **23**, 425–32 (2005).
21. Taipale, J. & Keski-Oja, J. Growth factors in the extracellular matrix. *FASEB J* **11**, 51–9 (1997).
22. Varghese, S. *et al.* Chondroitin sulfate based niches for chondrogenic differentiation of mesenchymal stem cells. *Matrix Biol* **27**, 12–21 (2008).
23. Francis, K. & Palsson, B. O. Effective intercellular communication distances are determined by the relative time constants for cyto/chemokine secretion and diffusion. *Proc Natl Acad Sci U S A* **94**, 12258–62 (1997).
24. Bian, L., Zhai, D. Y., Mauck, R. L. & Burdick, J. A. Coculture of human mesenchymal stem cells and articular chondrocytes reduces hypertrophy and enhances functional properties of engineered cartilage. *Tissue Eng Part A* **17**, 1137–45 (2011).
25. Yang, H. *et al.* The use of green fluorescence gene (GFP)-modified rabbit mesenchymal stem cells (rMSCs) co-cultured with chondrocytes in hydrogel constructs to reveal the chondrogenesis of MSCs. *Biomaterials* **30**, 6374–6385 (2009).
26. Liu, X. *et al.* In vivo ectopic chondrogenesis of BMSCs directed by mature chondrocytes. *Biomaterials* **31**, 9406–9414 (2010).
27. Wu, L., Prins, H. J., Helder, M. N., van Blitterswijk, C. A. & Karperien, M. Trophic effects of mesenchymal stem cells in chondrocyte co-cultures are independent of culture conditions and cell sources. *Tissue Eng Part A* **18**, 1542–51 (2012).
28. Tsuchiya, K., Chen, G., Ushida, T., Matsuno, T. & Tateishi, T. The effect of coculture of chondrocytes with mesenchymal stem cells on their cartilaginous phenotype in vitro. *Materials Science & Engineering C-Biomimetic and Supramolecular Systems* **24**, 391–396 (2004).
29. Levorson, E. J., Mountziaris, P. M., Hu, O., Kasper, F. K. & Mikos, A. G. Cell Derived Polymer/Extracellular Matrix Composite Scaffolds for Cartilage Regeneration, Part 1: Investigation of Co-cultures and Seeding Densities for Improved Extracellular Matrix Deposition. *Tissue Eng Part C Methods* DOI:10.1089/ten.tec.2013.0286 (2013).

30. Wu, L., Leijten, J., van Blitterswijk, C. A. & Karperien, M. Fibroblast growth factor-1 is a mesenchymal stromal cell-secreted factor stimulating proliferation of osteoarthritic chondrocytes in co-culture. *Stem Cells Dev* **22**, 2356–67 (2013).

31. Lee, J. S. & Im, G. I. Influence of chondrocytes on the chondrogenic differentiation of adipose stem cells. *Tissue Eng Part A* **16**, 3569–77 (2010).

32. Hildner, F. *et al.* Human Adipose-Derived Stem Cells Contribute to Chondrogenesis in Coculture with Human Articular Chondrocytes. *Tissue Engineering Part A* **15**, 3961–3969 (2009).

33. Hwang, N. S. *et al.* Response of zonal chondrocytes to extracellular matrix-hydrogels. *Febs Letters* **581**, 4172–4178 (2007).

34. Häuselmann, H. J. *et al.* Synthesis and turnover of proteoglycans by human and bovine adult articular chondrocytes cultured in alginate beads. *Matrix* **12**, 116–29 (1992).

35. Patwari, P. *et al.* Proteoglycan degradation after injurious compression of bovine and human articular cartilage in vitro: interaction with exogenous cytokines. *Arthritis Rheum* **48**, 1292–301 (2003).

36. Kim, T. K. *et al.* Experimental model for cartilage tissue engineering to regenerate the zonal organization of articular cartilage. *Osteoarthritis Cartilage* **11**, 653–64 (2003).

37. Rieck, B. Unexpected durability of PKH 26 staining on rat adipocytes. *Cell Biol Int* **27**, 445–7 (2003).

38. Osanai, T. *et al.* Noninvasive transplantation of bone marrow stromal cells for ischemic stroke: preliminary study with a thermoreversible gelation polymer hydrogel. *Neurosurgery* **66**, 1140–7; discussion 1147 (2010).

39. Horan, P. K. & Slezak, S. E. Stable cell membrane labelling. *Nature* **340**, 167–8 (1989).

40. Khetan, S. & Burdick, J. Patterning hydrogels in three dimensions towards controlling cellular interactions. *Soft Matter* **7**, 830–838 (2011).

41. Kaji, H., Camci-Unal, G., Langer, R. & Khademhosseini, A. Engineering systems for the generation of patterned co-cultures for controlling cell-cell interactions. *Biochimica Et Biophysica Acta-General Subjects* **1810**, 239–250 (2011).

42. Detamore, M. S. & Athanasiou, K. A. Effects of growth factors on temporomandibular joint disc cells. *Arch Oral Biol* **49**, 577–83 (2004).

43. Wang, C. Y. *et al.* Apoptosis in chondrogenesis of human mesenchymal stem cells: effect of serum and medium supplements. *Apoptosis* **15**, 439–49 (2010).

44. Dexheimer, V., Frank, S. & Richter, W. Proliferation as a requirement for in vitro chondrogenesis of human mesenchymal stem cells. *Stem Cells Dev* **21**, 2160–9 (2012).

45. Chen, L., Tredget, E. E., Wu, P. Y. & Wu, Y. Paracrine factors of mesenchymal stem cells recruit macrophages and endothelial lineage cells and enhance wound healing. *PLoS One* **3**, e1886 (2008).

46. Tang, Y. L. Paracrine action enhances the effects of autologous mesenchymal stem cell transplantation on vascular regeneration in rat model of myocardial infarction. *Ann Thorac Surg* **80**, 229–36; discussion 236–7 (2005).

47. Rehman, J. *et al.* Secretion of angiogenic and antiapoptotic factors by human adipose stromal cells. *Circulation* **109**, 1292–8 (2004).

48. Nakagami, H. *et al.* Novel autologous cell therapy in ischemic limb disease through growth factor secretion by cultured adipose tissue-derived stromal cells. *Arterioscler Thromb Vasc Biol* **25**, 2542–7 (2005).

49. Veilleux, N. & Spector, M. Effects of FGF-2 and IGF-1 on adult canine articular chondrocytes in type II collagen-glycosaminoglycan scaffolds in vitro. *Osteoarthritis Cartilage* **13**, 278–86 (2005).

50. Kato, Y. & Iwamoto, M. Fibroblast growth factor is an inhibitor of chondrocyte terminal differentiation. *J Biol Chem* **265**, 5903–9 (1990).

51. Martin, I. *et al.* Enhanced cartilage tissue engineering by sequential exposure of chondrocytes to FGF-2 during 2D expansion and BMP-2 during 3D cultivation. *J Cell Biochem* **83**, 121–8 (2001).

52. Kim, D. H. *et al.* Gene expression profile of cytokine and growth factor during differentiation of bone marrow-derived mesenchymal stem cell. *Cytokine* **31**, 119–26 (2005).

53. Rothenberg, A. R., Ouyang, L. & Elisseeff, J. H. Mesenchymal stem cell stimulation of tissue growth depends on differentiation state. *Stem Cells Dev* **20**, 405–14 (2011).

54. Schmittgen, T. D. & Livak, K. J. Analyzing real-time PCR data by the comparative C(T) method. *Nat Protoc* **3**, 1101–8 (2008).

55. Farndale, R. W., Buttle, D. J. & Barrett, A. J. Improved quantitation and discrimination of sulphated glycosaminoglycans by use of dimethylmethylene blue. *Biochim Biophys Acta* **883**, 173–7 (1986).

56. Stegemann, H. & Stalder, K. Determination of hydroxyproline. *Clin Chim Acta* **18**, 267–73 (1967).

57. Estes, B. T., Diekman, B. O., Gimble, J. M. & Guilak, F. Isolation of adipose-derived stem cells and their induction to a chondrogenic phenotype. *Nat Protoc* **5**, 1294–311 (2010).

Acknowledgments

Author contributions

"J.H.L. and F.Y. designed the study; J.H.L. and G.K. performed the research; J.H.L. and F.Y. made the figures and wrote the manuscript; J.H.L., F.Y., R.L.S. and W.M. reviewed and interpreted the data. All authors discussed the results and reviewed the manuscript."

Additional information